AUTOPHAGY
2020, VOL. 16, NO. 1, 70–85
https://doi.org/10.1080/15548627.2019.1598750

Taylor & Francis
Taylor & Francis Group

RESEARCH PAPER

Long noncoding RNA *CA7-4* promotes autophagy and apoptosis via sponging *MIR877-3P* and *MIR5680* in high glucose-induced vascular endothelial cells

Xuan Zhao[a], Le Su[a], Xiaoying He[a], Baoxiang Zhao[b], and Junying Miao[a,c]

[a]Shandong Provincial Key Laboratory of Animal Cells and Developmental Biology, School of Life Science, Shandong University, Jinan, P. R. China; [b]Institute of Organic Chemistry, School of Chemistry and Chemical Engineering, Shandong University, Jinan, P. R. China; [c]The Key Laboratory of Cardiovascular Remodeling and Function Research, Chinese Ministry of Education and Chinese Ministry of Health, Shandong University Qilu Hospital, Jinan, P. R. China

ABSTRACT

Vascular endothelial cells (VECs) that form the inner wall of blood vessels can be injured by high glucose-induced autophagy and apoptosis. Although the role of long noncoding RNA in regulating cell fate has received widespread attention, long noncoding RNAs (lncRNAs) that can both regulate autophagy and apoptosis need to be discovered. In this study, we identified that a small chemical molecule, 3-benzyl-5-([2-nitrophenoxy] methyl)-dihydrofuran-2(3H)-one (3BDO), synthesized by us, could inhibit VEC autophagy and apoptosis induced by a high concentration of glucose. To find new lncRNAs that regulate autophagy and apoptosis in VECs, we performed lncRNA microarray analysis. We found and verified an upregulated lncRNA named *CA7-4* that was induced by a high concentration of glucose could be downregulated by 3BDO most obviously among all of the detected lncRNAs. Meanwhile, we investigated the mechanism of *CA7-4* in regulating VEC autophagy and apoptosis. The results showed that *CA7-4* facilitated endothelial autophagy and apoptosis as a competing endogenous RNA (ceRNA) by decoying *MIR877-3P* and *MIR5680*. Further study elucidated that *MIR877-3P* could trigger the decrease of CTNNBIP1 (catenin beta interacting protein 1) by combining with its 3′ UTR and then upregulating CTNNB1 (catenin beta 1); *MIR5680* inhibited the phosphorylation of AMP-activated protein kinase (AMPK) by targeting and decreasing DPP4 (dipeptidyl peptidase 4). Therefore, *CA7-4, MIR877-3P* and *MIR5680* represent new signal pathways that regulate VEC autophagy and apoptosis under the high-glucose condition.

ARTICLE HISTORY
Received 2 March 2018
Revised 3 March 2019
Accepted 15 March 2019

KEYWORDS
Apoptosis; autophagy; high glucose; lncRNA; miRNA; vascular endothelial cells

Abbreviations: 3BDO: 3-benzyl-5-([2-nitrophenoxy] methyl)-dihydrofuran-2(3H)-one; 3′ UTR: 3′ untranslated region; AGO2: argonaute RISC catalytic component 2; AMPK: AMP-activated protein kinase/protein kinase AMP-activated; BAX/BCL2L4: BCL2 associated X, apoptosis regulator; BCL2: BCL2 apoptosis regulator; CASP3: caspase 3; ceRNA: competing endogenous RNA; CTNNB1: catenin beta 1; CTNNBIP1/ICAT: catenin beta interacting protein 1; DPP4: dipeptidyl peptidase 4; FGF2/FGF-2: fibroblast growth factor 2; HG: high concentration glucose (30 mM glucose); lncRNA: long noncoding RNA; MAP1LC3B/LC3B: microtubule associated protein 1 light chain 3 beta; miRNA: microRNA; *MIR4778-3P*: microRNA 4778-3p; *MIR561-3P*: microRNA 561-3p; *MIR5680*: microRNA 5680; *MIR877-3P*: microRNA 877-3p; MTOR: mechanistic target of rapamycin kinase; Mut: mutant; NC: negative control; NG: normal concentration glucose (5.5 mM glucose); PARP1: poly(ADP-ribose) polymerase 1; qPCR: quantitative real-time PCR; RNA-FISH: RNA-fluorescence in situ hybridization; ROS: reactive oxygen species; RT-PCR: reverse transcription polymerase chain reaction; siRNA: small interfering RNA; SQSTM1: sequestosome 1; *TGFB2-OT1*: TGFB2 overlapping transcript 1; TUNEL: terminal deoxynucleotidyl transferase dUTP nick end labeling; VECs: vascular endothelial cells; WT: wild type

Introduction

A high concentration of glucose in the blood is harmful to vascular endothelial cells (VECs) [1]. Under hyperglycemia, the synthesis of nitric oxide (NO) decreases and reactive oxygen species (ROS) levels notably increase due to the inactivation of endothelial NO synthase. High glucose-induced oxidative stress induces cell death, impairs angiogenesis, and then leads to vascular diseases [1,2]. In parallel, studies have focused on investigating the mechanism of endothelial cell autophagy, apoptosis, inflammation and senescence induced by high glucose. For instance, the production of ROS induced by hyperglycemia contributes to caspase-dependent apoptosis of endothelial cells by triggering CYCS (cytochrome c, somatic) release [3]. The chronic elevation of glucose level promotes the expression of various inflammatory factors in endothelial cells, including ICAM1 (intercellular adhesion molecule 1), IL6 (interleukin 6) [4], and VCAM1 (vascular cell adhesion molecule 1) [5]. In addition, high glucose accelerates endothelial cell senescence, apoptosis and autophagy by inducing renin-angiotensin system-mitochondrial damage [6].

CONTACT Junying Miao miaojy@sdu.edu.cn Shandong Provincial Key Laboratory of Animal Cells and Developmental Biology, School of Life Science, Shandong University, Jinan 250100, P. R. China
Supplemental data for this article can be accessed here.

Consequently, exploring novel regulatory factors to reduce the injury caused by hyperglycemia on endothelial cells is of great significance.

Only about 2% of sequences of human genome can be translated into protein. Transcripts that do not encode a protein can be divided according to length, including short non-coding RNAs (<200 nt) and long non-coding RNAs (lncRNAs, >200 nt) [7]. However, these noncoding transcripts do not simply exist as trash or transcriptional noise [8]. LncRNAs have been extensively considered critical players in regulating dosage compensation, genomic imprinting, chromatin remodeling, DNA methylation, cell differentiation, organogenesis, and the physiological and pathological processes of organisms [9]. Beyond that, many reports demonstrate that lncRNAs are emerging as central regulators in controlling cell autophagy or apoptosis of various diseases, including cancers [10–12], cardiovascular diseases [13–15], and diabetic vascular complications [16].

Nevertheless, only a few studies have investigated lncRNA regulation in endothelium injury caused by hyperglycemia. For example, under high glucose, *MALAT1* (metastasis associated lung adenocarcinoma transcript 1) knockdown ameliorates retinal vessel apoptosis and capillary impairment [17]; *MEG3* (maternally expressed 3) knockdown aggravates retinal vascular dysfunction [18]; *MIAT* (myocardial infarction associated transcript) is involved in regulating retinal vessel dysfunction as the decoy of *MIR150-5P* [19]; and *CDKN2B-AS1* (CDKN2B antisense RNA 1) promotes angiogenesis by upregulating VEGFA/VEGF (vascular endothelial growth factor A) and activating NFKB1 (nuclear factor kappa B subunit 1) signaling [20].

MicroRNAs (miRNAs) also play important roles in endothelial injury induced by hyperglycemia. In general, these are a class of evolutionarily conserved non-coding RNAs approximately 20–22 nt in length. Accumulating evidence has revealed that miRNAs, alone or in combination with lncRNAs, are involved in regulating specific gene expression at the transcription or translation level, then changing cell signaling pathways associated with different physiological and pathological processes [21]. For the past few years, studies have elevated our understanding of miRNA regulation in hyperglycemia-induced endothelial dysfunction. For example, *MIR126* inhibits inflammation and ROS production by targeting HMGB1 (high-mobility group box 1) in diabetic vascular endothelium [22]; overexpression of *MIR149-5P* improves high glucose-induced VEC dysfunction and apoptosis by targeting and downregulating TNF/TNFα (tumor necrosis factor) [23]. Consequently, noncoding RNAs, including lncRNAs and miRNAs, are emerging as diagnostic biomarkers or therapeutic targets of diabetes-associated vascular complications because of their regulation of endothelial injury induced by high glucose [24].

Our previous study indicates that a small chemical molecule, 3BDO, inhibits serum and FGF2 (fibroblast growth factor 2) deprivation-induced VEC apoptosis [25]. In 2014, we have identified that 3BDO inhibits autophagy as a novel activator of MTOR (mechanistic target of rapamycin kinase) and also found a new lncRNA, *TGFB2-OT1* (TGFB2 overlapping transcript 1), that regulates autophagy in VECs by decoying *MIR4459* targeting ATG13 (autophagy-related 13), and 3BDO reduces *TGFB2-OT1* by promoting the phosphorylation of TIA1 (TIA1 cytotoxic granule associated RNA binding protein) [26]. Furthermore, 3BDO ameliorates autophagy and inflammation of VECs caused by lipopolysaccharide and oxidized low-density lipoprotein through diminishing *TGFB2-OT1* [27]. Thus, according to the available evidence, we speculated that 3BDO may both suppress endothelial autophagy and apoptosis induced by high glucose.

In this study, we first demonstrated that 3BDO could alleviate high glucose-induced VEC autophagy and apoptosis and also identified a new lncRNA named *CA7-4* by high-throughput sequencing. Here, 3BDO could decrease the level of *CA7-4*. Additionally, our findings highlighted novel miRNA signal pathways regulated by *CA7-4* in autophagy and apoptosis of VECs.

Results

3BDO restrained the upregulation of *CA7-4* induced by high glucose in VECs

First, we found that 3BDO inhibited high glucose-induced VEC autophagy and apoptosis (Figure S1). However, the data revealed that 3BDO decreased high glucose-induced autophagy in VECs without a remarkable effect on the expression of SQSTM1 (sequestosome 1) (Figure S1(c)). To investigate novel lncRNAs participating in VEC autophagy and apoptosis under high glucose, we performed lncRNA microarray analysis after treating VECs with normal concentration glucose (5.5 mM glucose) (NG), high concentration glucose (30 mM glucose) (HG), and HG+3BDO (60 μM) (Figure 1(a)) and found a new lncRNA, *CA7-4*, prominently regulated by HG+3BDO (Figure 1(b)). We examined the expression of *CA7-4* by quantitative real-time PCR (qPCR) after treatment with high glucose or 3BDO. 3BDO inhibited the upregulated *CA7-4* caused by high glucose (Figure 1(d,e)). Under normal glucose, 3BDO still could downregulate *CA7-4* (Figure 1(f)).

In the LNCipedia database (version 5.2), *CA7-4* has been identified as an lncRNA (https://lncipedia.org/db/transcript/lnc-CA7-4:1). It is located in the forward strand of chromosome 16 (hg38), is 2894 bp in full length, consists of two exons and one intron, and is antisense to *DYNC1LI2* (dynein cytoplasmic 1 light intermediate chain 2) and *TERB1* (telomere repeat binding bouquet formation protein 1) (Figure 1(c)). However, no one has studied the function of *CA7-4*. First, we analyzed the expression pattern of *CA7-4* in different human cell lines (Figure S2(a)) and found *CA7-4* expressed highly in VEC, Hela and A549 cells. Then we predicted the subcellular localization of *CA7-4* via http://www.csbio.sjtu.edu.cn/bioinf/lncLocator (Figure S2(b)). RNA-fluorescence in situ hybridization (RNA-FISH) and nuclear/cytoplasmic RNA separation analysis revealed that *CA7-4* distributed in both nucleus and cytoplasm of VECs (Figure S2(c,d)). Moreover, HG increased the RNA level of *CA7-4* in the cytoplasm instead of the nucleus (Figure S2(e)). After treatment with 3BDO, the distribution of *CA7-4* in the cytoplasm was significantly reduced(Figure S2(f,g)).

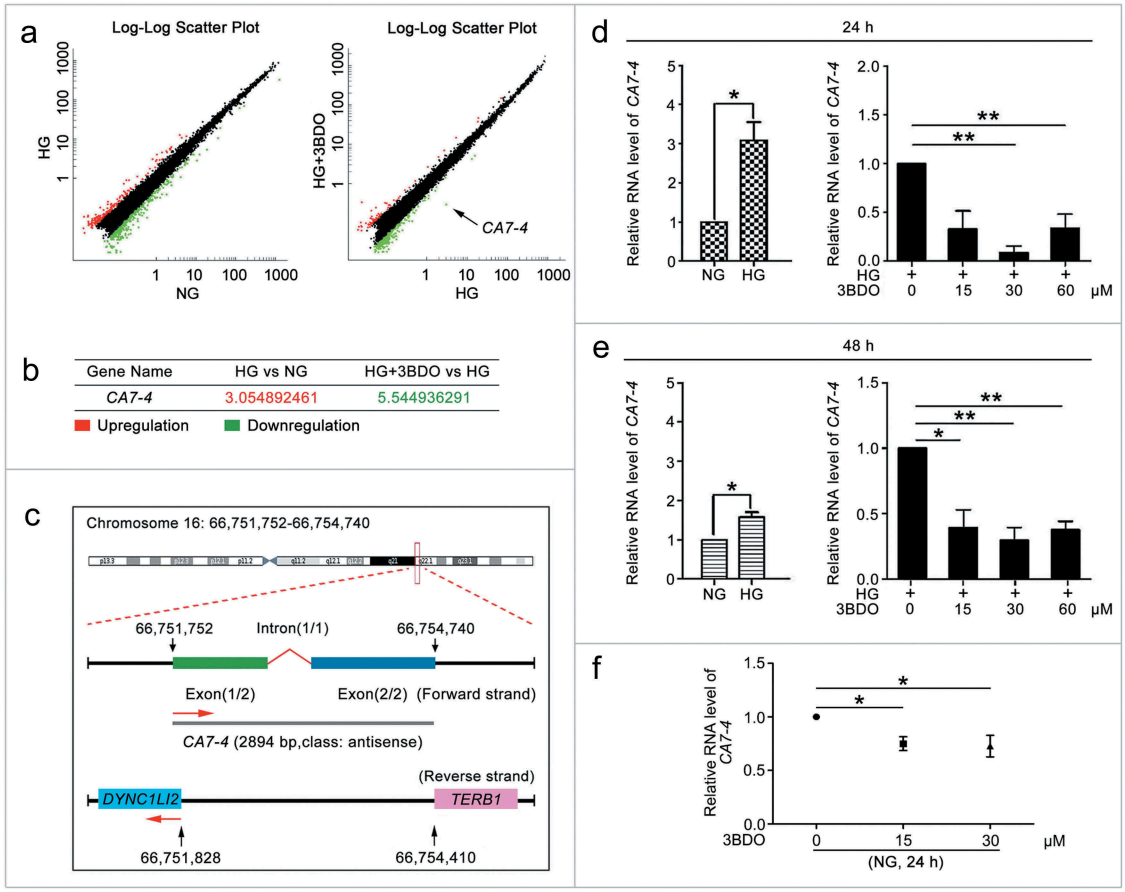

Figure 1. 3BDO could suppress the increase in *CA7-4* expression caused by high glucose. (a) The scatter plot of microarray analysis depicts genes upregulated (red) and downregulated (green). *CA7-4* level was decreased obviously, as indicated by the arrow. (b) Changes in *CA7-4* level with treatment. (c) Information on *CA7-4* in the human genome is available at https://lncipedia.org/db/transcript/lnc-CA7-4:1. (d,e) VECs were treated with 5.5 mM glucose (NG), 30 mM glucose (HG), and HG+3BDO (15, 30, 60 μM) for 24 h and 48 h. (f) VECs were treated with NG, 3BDO (0, 15, 30 μM) for 24 h. The level of *CA7-4* was detected by qPCR. (*, $p < 0.05$; **, $p < 0.01$; $n = 3$.).

Overexpression *CA7-4* promoted high glucose-induced VEC autophagy

To clarify the function of *CA7-4* in VECs, we cloned full-length *CA7-4* into the pcDNA3.1 plasmid (pcDNA3.1-*CA7-4*) and synthesized specific siRNAs against *CA7-4*. Then the overexpression and interference efficiency of *CA7-4* was assessed by qPCR analysis (Figure 2(a,b)). In VECs, after overexpression of *CA7-4* and treatment with high glucose, we detected the distribution of LC3B (microtubule associated protein 1 light chain 3 beta) by immunofluorescence. *CA7-4* substantially increased LC3B puncta and the protein level of LC3B-II in VECs with high glucose treatment (Figure 2(c,d)) and without high glucose treatment (Figure 2(e)). 3BDO inhibited the upregulation of LC3B-II induced by *CA7-4* (Figure 2(f)). Thus, *CA7-4* aggravated VEC autophagy. We found that cells containing a large number of autophagosomes were also accompanied with nuclear shrinkage, so *CA7-4* may also regulate VEC apoptosis.

High glucose-induced VEC apoptosis was aggravated by *CA7-4*

To detect whether *CA7-4* affected VEC apoptosis, we treated cells with high glucose after transfection with *CA7-4* and si-*CA7-4*. *CA7-4* heightened the levels of BAX and cleaved-PARP1 (Figure 3(a,b)); these observations could be reversed by *CA7-4* knockdown (Figure 3(c,d)). Then we used Hoechst 33258 staining analysis after overexpression of *CA7-4* and found that *CA7-4* favored VEC apoptosis (Figure 3(e)). Also, *CA7-4* increased the level of cleaved-CASP3 in VECs, whereas *CA7-4* knockdown reversed the result (Figure 3(f)). Hence, *CA7-4* increased VEC apoptosis directly.

CA7-4 decoyed *MIR877-3P* and *MIR5680* as a sponge RNA

Studies have shown that lncRNAs affect mRNA stability by competing endogenous RNAs (ceRNAs) [28]. To determine the mechanism of *CA7-4* boosting autophagy and apoptosis in VECs, we predicted miRNAs that may combine with *CA7-4* by bioinformatics analysis (http://starbase.sysu.edu.cn/mirLncRNA.php) and found *MIR877-3P, MIR5680, MIR4778-3P, MIR561-3P* with higher binding scores. *CA7-4* overexpression decreased the levels of these miRNAs (Figures 4(a,c), S3(a,c)), whereas *CA7-4* knockdown elevated the levels (Figures 4(b,d), S3(b,d)), and 3BDO promoted the expression of *MIR877-3P* and *MIR5680* especially (Figure 4(e–h)). Furthermore, we predicted the possible sites for *MIR877-3P, MIR5680, MIR4778-3P*, and *MIR561-3P* bonding with *CA7-4*,

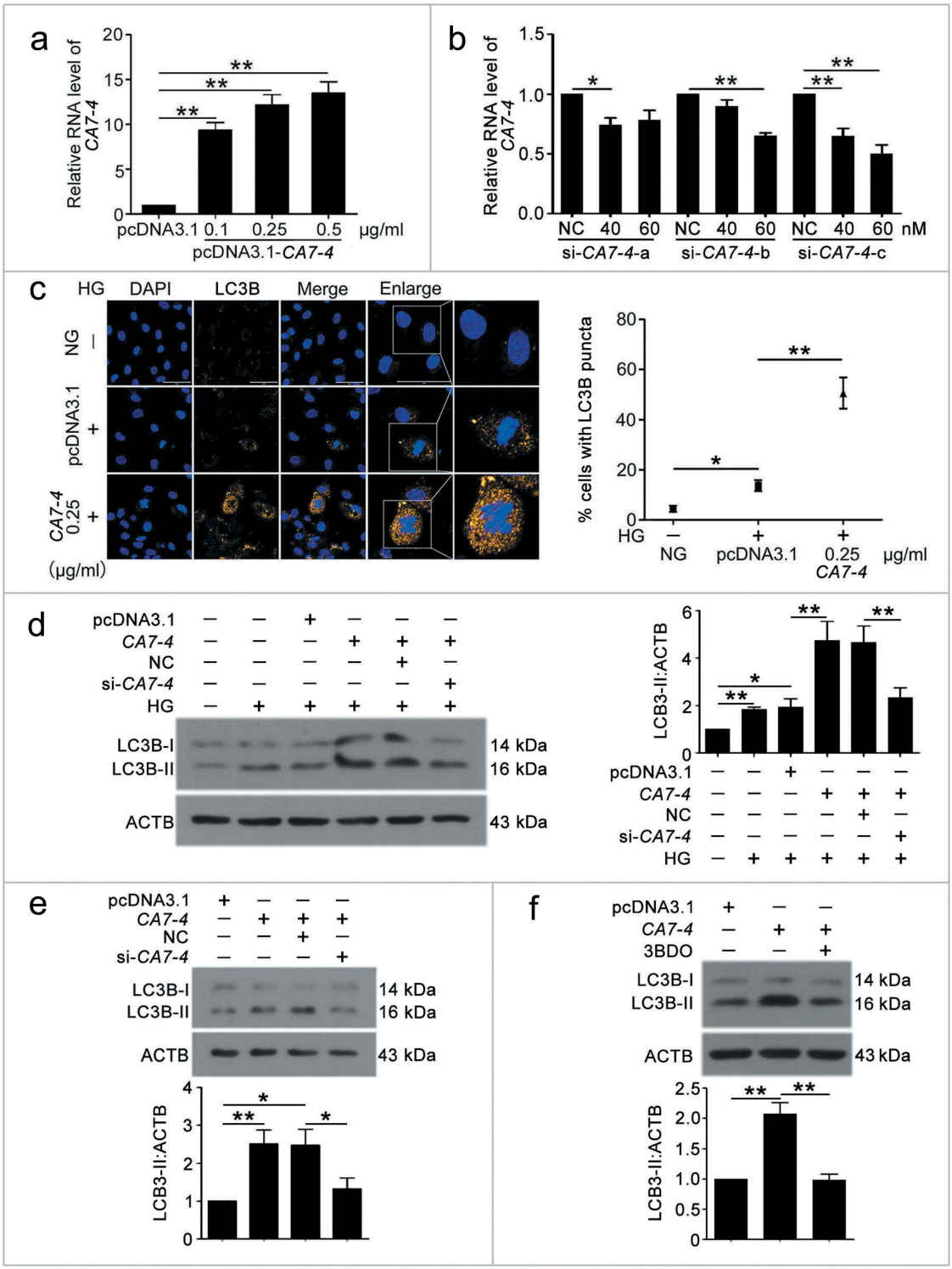

Figure 2. *CA7-4* encouraged VEC autophagy. (a) VECs were transfected with empty vector pcDNA3.1 and *CA7-4* (0.1, 0.25, 0.5 μg/ml) for 48 h. qPCR analysis of *CA7-4* overexpression efficiency. (b) VECs were transfected with NC or siRNA-*CA7-4*-a, siRNA-*CA7-4*-b, and siRNA-*CA7-4*-c for 48 h. qPCR analysis of the RNA level of *CA7-4*. (c) After transfection with pcDNA3.1 or *CA7-4* (0.25 μg/ml) for 24 h, VECs were treated with HG for 48 h. The distribution of LC3B in VECs was detected by immunofluorescence, and the proportion of cells containing > 5 LC3B puncta was investigated. Scale bar: 50 μm. Rescue experiment: VECs were transfected with pcDNA3.1 or *CA7-4*, then co-transfected with *CA7-4* (0.1 μg/ml) and NC; *CA7-4* (0.1 μg/ml) and si-*CA7-4* (60 nM) for 24 h (d) or 48 h (e), then treated with HG (d) for 48 h. (f) VECs were treated with 3BDO (15 μM) for 48 h after transfection with *CA7-4* (0.1 μg/ml) overnight. Western blot analysis of LC3B-II level. (*, $p < 0.05$; **, $p < 0.01$; $n = 3$.).

with putative sites at positions 1302 to 1322, 863 to 884, 2316 to 2337 and 2323 to 2344, respectively. Luciferase activity was reduced after co-transfection with Luc-*CA7-4*-WT plasmid and *MIR877-3P* or *MIR5680* mimics into HEK293T cells as compared with the negative control or plasmids containing the mutant sequences of presumptive binding sites (Figure 4(i,j)). However, luciferase activity did not differ after co-transfection with Luc-*CA7-4*-WT plasmid and *MIR4778-3P* or *MIR561-3P*

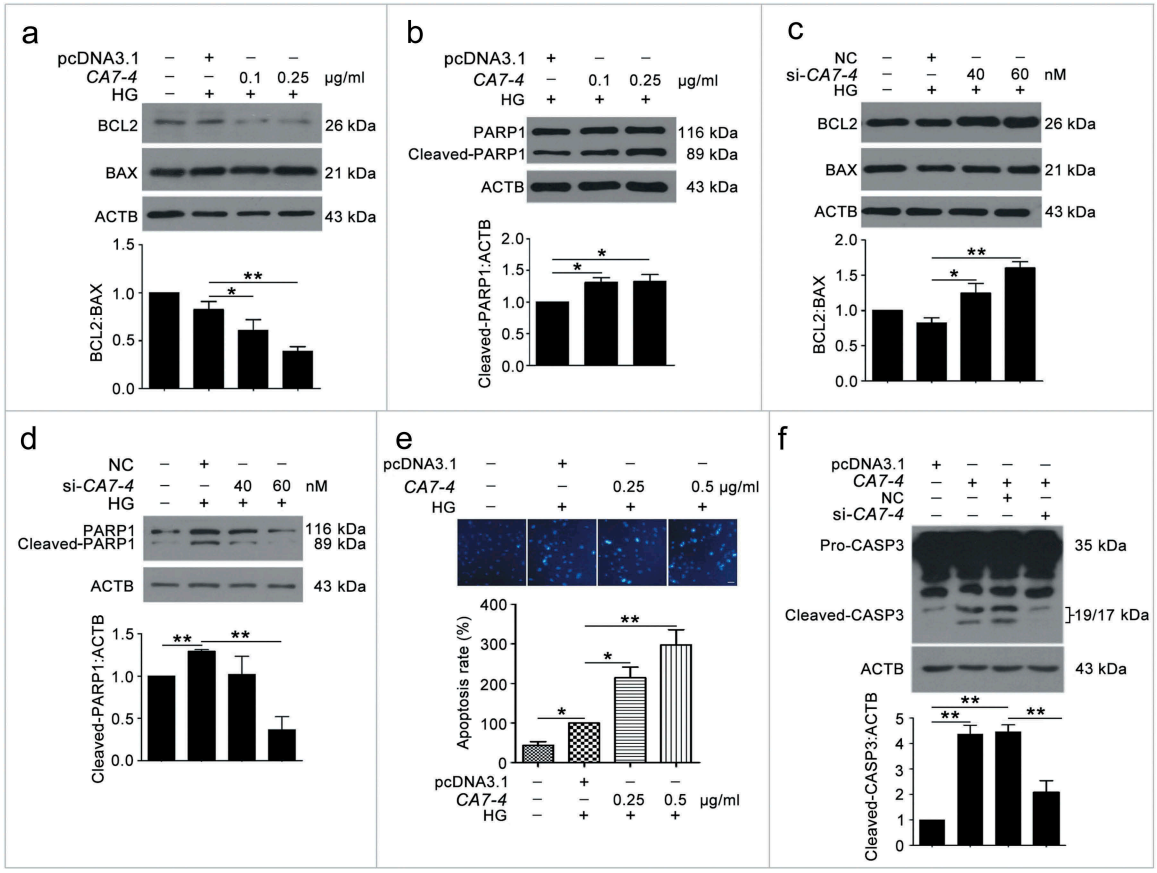

Figure 3. Overexpressing *CA7-4* increased VEC apoptosis. (a–d) After being transfected with pcDNA3.1 or *CA7-4*; NC or si-*CA7-4* overnight, VECs were treated with HG for 48 h, and the protein levels of BCL2, BAX and cleaved-PARP1 were detected by western blot. (e) VECs were treated with HG for 48 h after overexpression of *CA7-4*. Hoechst 33258 staining analysis of cell apoptosis. Scale bar: 30 μm. (f) VECs were transfected with pcDNA3.1 or *CA7-4*; co-transfected with *CA7-4* (0.1 μg/ml) and NC or si-*CA7-4* (60 nM) for 48 h. The level of cleaved-CASP3 was detected by western blot. (*, $p < 0.05$; **, $p < 0.01$; $n = 3$.).

mimics as compared with the negative control (Figure S3(e,f)). As we know, microRNAs fail to modulate target mRNAs when ceRNAs bind to microRNA-induced silencing complex (RISC) as microRNA sponges [29]. AGO2 (argonaute RISC catalytic component 2) is the core component of RISC, RNA-binding protein immunoprecipitation (RIP) experiment demonstrated the existence of *CA7-4* in the anti-AGO2 group under the treatments of NG, 3BDO, HG, HG+3BDO (Figure 4(k–m)), and 3BDO conspicuously decreased the enrichment of *CA7-4* in AGO2 (Figure 4(l,m)). So, *CA7-4* directly combined with *MIR877-3P* and *MIR5680* as a miRNA decoy.

MIR877-3P and *MIR5680* suppressed VEC autophagy and apoptosis

To understand the mechanism of *CA7-4* regulating VEC autophagy and apoptosis, we considered *MIR877-3P* and *MIR5680* as the point of penetration. First, RNA-FISH revealed that *MIR877-3P* and *MIR5680* distributed in both nucleus and cytoplasm of VECs (Figure S4). Next, we transfected VECs with *MIR877-3P* and *MIR5680* mimics or inhibitor overnight and then incubated cells with high glucose. LC3B-II level and LC3B immunofluorescence indicated that *MIR877-3P* (Figure 5(a,b)) and *MIR5680* (Figure 6(a–c)) protected VECs against high glucose-caused autophagy. Simultaneously, according to TUNEL assay and Hoechst 33258 staining, *MIR877-3P* (Figure 5(c–e)) and *MIR5680* (Figure 6(d)) alleviated VEC apoptosis. Furthermore, in normal cultured VECs, *MIR877-3P* (Figure S6) and *MIR5680* (Figure S7) had a parallel effect on autophagy and apoptosis. Therefore, *MIR877-3P* and *MIR5680* weakened VEC autophagy and apoptosis directly.

MIR877-3P and *MIR5680* targeted the 3′ UTRs of *CTNNBIP1* and *DPP4* respectively

Because *CA7-4* increased VEC autophagy and apoptosis by sponging *MIR877-3P* and *MIR5680*, we predicted the possible targets of *MIR877-3P* and *MIR5680* via miRDB-MicroRNA Target Prediction and Functional Study Database (http://www.mirdb.org/). Among the predicted target genes of *MIR877-3P* and *MIR5680*, *CTNNBIP1* (catenin beta interacting protein 1) and *DPP4* (dipeptidyl peptidase 4) strongly drew our attention (Table S1). CTNNBIP1 injures T-cell development by contributing to T-cell apoptosis and destroying the interactions between CTNNB1 (catenin beta 1) and T-cell factor [30]. However, we have no data on the association between CTNNBIP1 and autophagy. Research has illuminated that inhibitors of

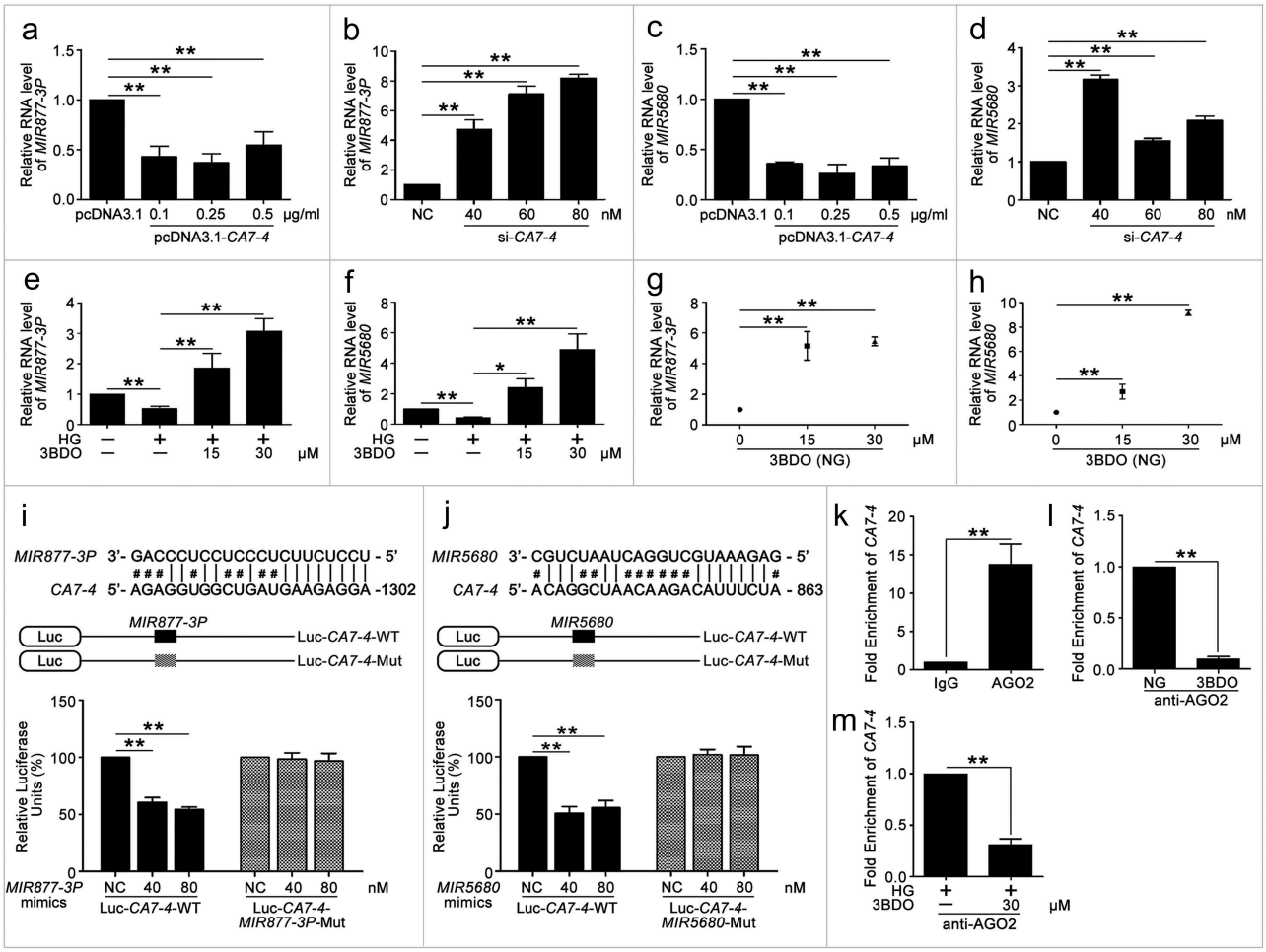

Figure 4. *CA7-4* directly bonded with *MIR877-3P* and *MIR5680*. (a–d) qPCR analysis of *MIR877-3P* and *MIR5680* in VECs after overexpression or knockdown *CA7-4* for 48 h. (e–h) VECs were treated with NG, HG, HG+3BDO, or 3BDO (NG) for 24 h, qPCR analysis of *MIR877-3P* and *MIR5680*. (i,j) Luc-*CA7*-WT, Luc-*CA7-4-MIR877-3P*-Mut, and Luc-*CA7-4- MIR5680*-Mut plasmids were separately co-transfected into HEK293T cells with NC, *MIR877-3P* mimics or *MIR5680* mimics for 24 h. Detecting luciferase activity. (k–m) RNA binding protein immunoprecipitation experiments were performed by using AGO2 antibody in VECs after treatment with NG, 3BDO (30 μM), HG and HG+3BDO (30 μM) for 24 h. IgG was used as a negative control. The fold enrichment of pulled-down *CA7-4* was detected by qPCR analysis. (*, $p < 0.05$; **, $p < 0.01$; $n = 3$.).

DPP4 show excellent anti-hyperglycemic performance, superior to traditional treatment, especially for older people and women [31]. Moreover, as one of the DPP4 inhibitors, sitagliptin contributes to protect mesenchymal stem cells against hypoxia-induced apoptosis and autophagy [32]. Therefore, we explored whether *MIR877-3P* and *MIR5680* targeted and affected CTNNBIP1 and DPP4, respectively.

We found that positions 2368 to 2388 contained the binding sites of *MIR877-3P* and *CTNNBIP1* 3′ UTR (Figure 7(a)). Likewise, according to the prediction results, *MIR5680* has two putative *DPP4* 3′ UTR binding sites at positions 225 to 246 and 845 to 866 (Figure 8(a)). Luciferase assays showed that *MIR877-3P* mimics co-transfection with Luc-*CTNNBIP1* 3′ UTR-WT plasmid repressing luciferase activity significantly as compared with transfection of the negative control or Luc-*CTNNBIP1* 3′ UTR-Mut (Figure 7(b)). Also, *MIR5680* mimics weakened luciferase activity of Luc-*DPP4* 3′UTR-WT instead of Luc-*DPP4* 3′ UTR-Mut (Figure 8(b)). Hence, *MIR877-3P* and *MIR5680* directly targeted *CTNNBIP1* and *DPP4* 3′ UTRs, respectively.

MIR877-3P, MIR5680 and 3BDO separately downregulated CTNNBIP1 and DPP4; *CA7-4* upregulated CTNNBIP1 and DPP4 by sponging *MIR877-3P* and *MIR5680*

We investigated whether *MIR877-3P* and *MIR5680* affected CTNNBIP1 and DPP4 expression. The protein level of CTNNBIP1 was promoted by *MIR877-3P* inhibitor but decreased by *MIR877-3P* mimics under high glucose (Figure 7(c)). Additionally, *MIR877-3P* mimics downregulated the mRNA level of *CTNNBIP1*, whereas overexpression *CA7-4* abolished this downregulation (Figure 7(d)). In normal VECs, *MIR877-3P* mimics (Figure 7(e)) inhibited the protein level of CTNNBIP1, whereas the *MIR877-3P* inhibitor (Figure 7(f)) and *CA7-4* increased it (Figure 7(g)). Additionally, *MIR5680* mimics decreased the expression of DPP4 at the levels of transcription

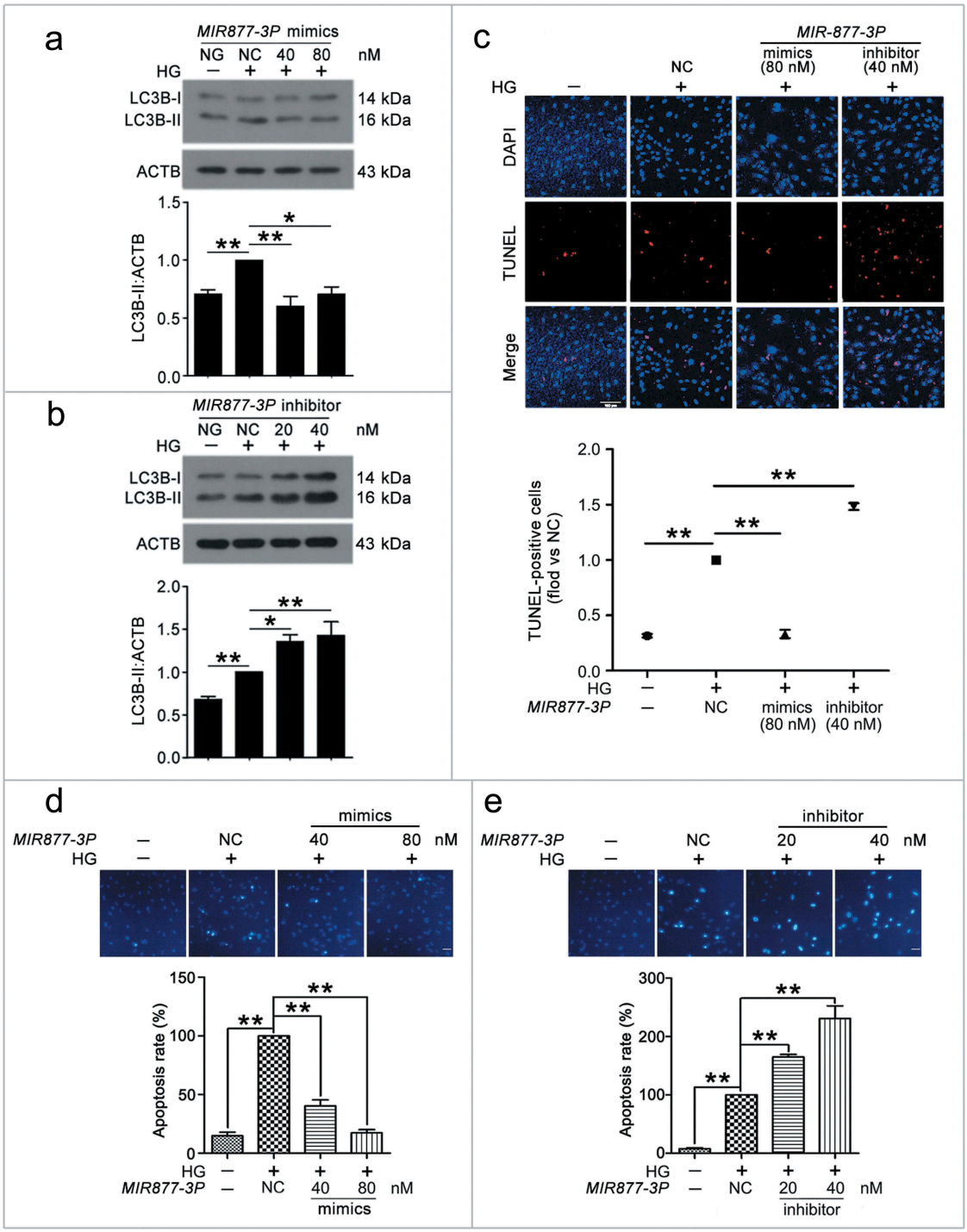

Figure 5. *MIR877-3P* inhibited VEC autophagy and apoptosis. After transfection with *MIR877-3P* mimics or inhibitor overnight, VECs were treated with HG for 48 h. (a, b) Western blot analysis of LC3B-II level. (c) TUNEL staining analysis of cell apoptosis. Scale bar: 100 μm. (d,e) Cell apoptosis was detected by Hoechst 33258 staining. Scale bar: 30 μm. (*, $p < 0.05$; **, $p < 0.01$; n = 3.).

(Figure 8(c)) and translation with or without high glucose treatment (Figure 9(a,d)). *MIR5680* inhibitor (Figure 9(b,e)) or *CA7-4* (Figures 8(d), 9(c)) transfection had the opposite results. As well, elevated CTNNBIP1 and DPP4 levels caused by high glucose decreased after treatment with siRNA-*CA7-4* or 3BDO (Figure S8). Therefore, we verified that *MIR877-3P*, *MIR5680*, 3BDO negatively modulated and *CA7-4* promoted the expression of CTNNBIP1 and DPP4.

CTNNBIP1 and DPP4 aggravated VEC autophagy and apoptosis under high glucose by inhibiting CTNNB1 expression and improving AMPK phosphorylation, respectively

CTNNBIP1 works as a key negative regulator of CTNNB1 and affects cell fate [33]. Thus, we analyzed whether *MIR877-3P* regulated the level of CTNNB1. After transfecting VECs with *MIR877-3P* mimics or inhibitor, we detected

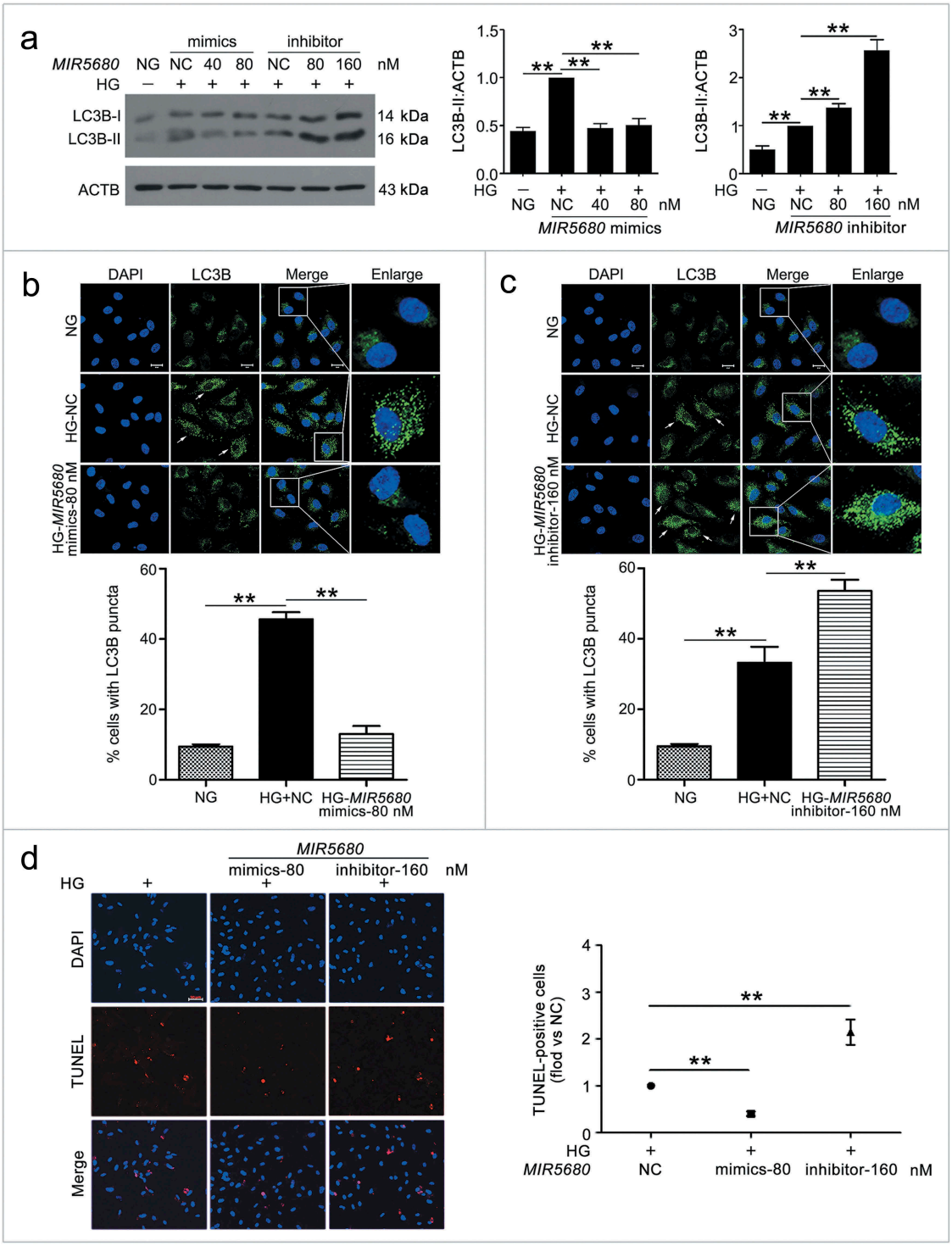

Figure 6. *MIR5680* prevented VEC autophagy and apoptosis. VECs were treated with HG for 48 h after transfection with *MIR5680* mimics or inhibitor overnight. (a) Western blot analysis of LC3B-II level. (b,c) Immunofluorescence analysis of the distribution of LC3B in VECs, and the proportion of cells containing > 5 LC3B puncta was analyzed. Scale bar: 20 μm. (d) TUNEL staining analysis of cell apoptosis. Scale bar: 50 μm. (*, $p < 0.05$; **, $p < 0.01$; n = 3.).

the protein level of CTNNB1 (Figure S9(a)) and found that *MIR877-3P* enhanced CTNNB1 expression. We also conducted a rescue experiment to explore whether *CA7-4* affected the expression of CTNNB1. High glucose and overexpression of *CA7-4* negatively regulated CTNNB1, but the protein level of CTNNB1 recovered after knockdown *CA7-4*, transfection with *MIR877-3P* mimics or treatment with 3BDO (Figure S9(b–d)).

AMPK regulates cellular metabolism as an energy sensor, and its activation leads to β-cell apoptosis [34]. In addition, AMPK is famous for activating autophagy to control cellular energy homeostasis through the AMPK/MTOR pathway [35]. Here, we hypothesized that *MIR5680* may have an impact on AMPK phosphorylation by restraining the expression of DPP4, then regulating autophagy in VECs. The data revealed that *MIR5680* suppressed AMPK phosphorylation (Figure S10).

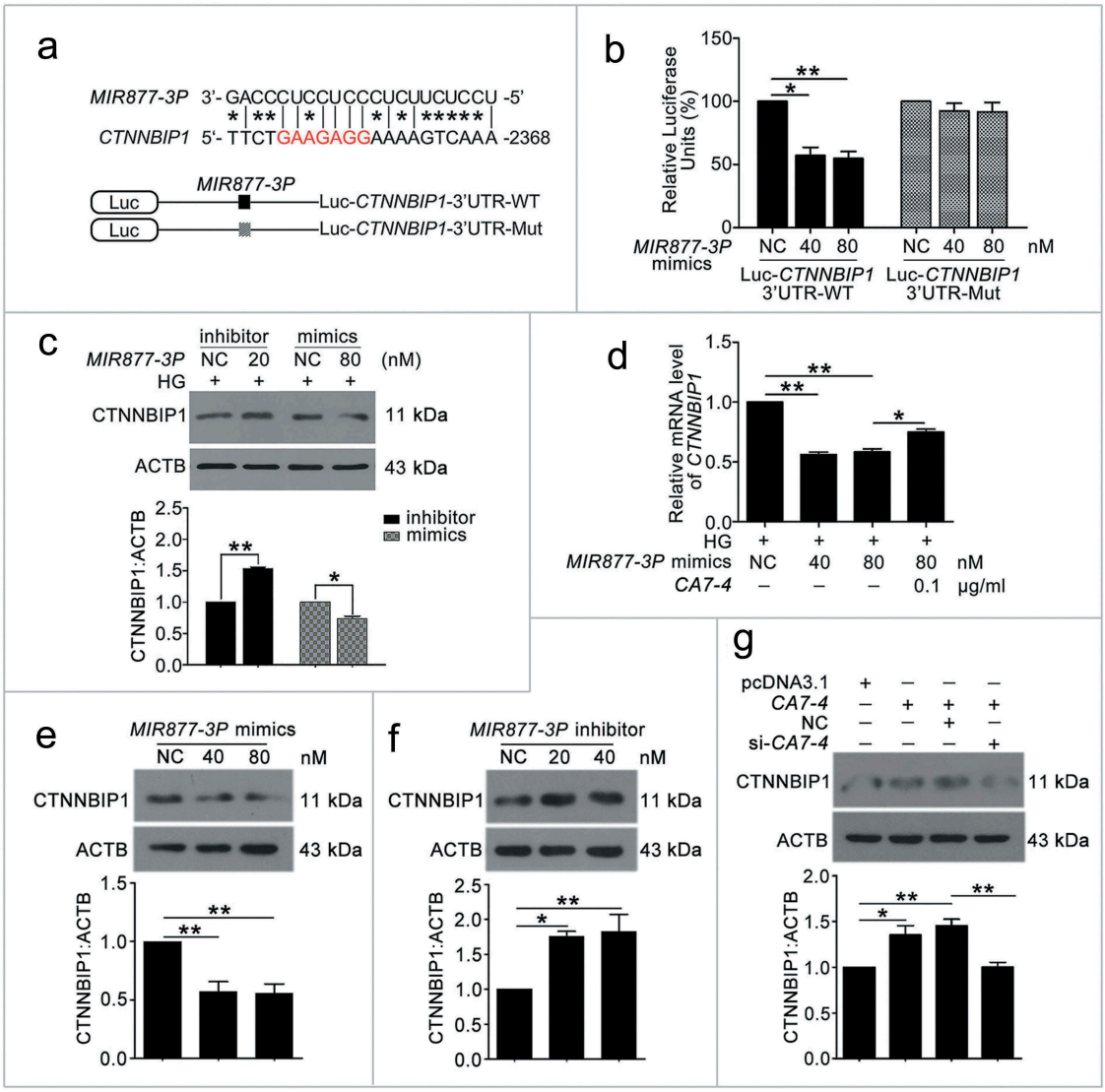

Figure 7. *MIR877-3P* targeted and inhibited CTNNBIP1. (a) Potential bind sites of *MIR877-3P* in *CTNNBIP1* 3′ UTR. (b) Luc-*CTNNBIP1* 3′ UTR-WT or Luc-*CTNNBIP1* 3′ UTR-Mut plasmid was co-transfected with NC or *MIR877-3P* mimics into HEK293T cells for 24 h. Luciferase activity was determined. (c) After transfection with NC, *MIR877-3P* inhibitor or mimics overnight, VECs were treated with HG for 48 h. Western blot analysis of CTNNBIP1. (d) VECs were treated with HG for 48 h after transfection with *MIR877-3P* mimics or co-transfection with *MIR877-3P* mimics and *CA7-4*. qPCR analysis of *CTNNBIP1* mRNA level. (e,f) VECs were transfected with NC, *MIR877-3P* mimics or inhibitor for 48 h. (g) VECs were transfected with pcDNA3.1 or *CA7-4* (0.1 μg/ml); co-transfected with *CA7-4* (0.1 μg/ml) and NC or si-*CA7-4* (60 nM) for 48 h. Western blot analysis of CTNNBIP1. (*, $p < 0.05$; **, $p < 0.01$; $n = 3$.).

Also, we found that *CA7-4* overexpression-upregulated AMPK phosphorylation could be abolished by 3BDO (Figure S10(c)).

To verify the roles of CTNNBIP1 and DPP4 in high glucose-induced VEC autophagy and apoptosis, we used siRNA knockdown and examined the protein levels of CTNNBIP1, CTNNB1, DPP4, p-AMPK, cleaved-CASP3, and LC3B-II (Figure 10). The results suggested that CTNNBIP1 reduced CTNNB1 expression and DPP4 promoted AMPK phosphorylation to enhance VEC autophagy and apoptosis.

In conclusion, high glucose-induced *CA7-4* upregulation, VEC autophagy and apoptosis could be inhibited by the small chemical molecule 3BDO. As a competing endogenous RNA, *CA7-4* decoyed *MIR877-3P* and *MIR5680*. *MIR877-3P* and *MIR5680* protected VECs against high glucose-caused autophagy and apoptosis by targeting the 3′ UTRs of *CTNNBIP1* and *DPP4*, negatively regulating their levels, as well as promoting the expression of CTNNB1 and downregulating AMPK phosphorylation (Figure 11).

Discussion

Normal endothelium function is essential for vascular homeostasis and remodeling. For decades, hyperglycaemia induced by diabetes has been reported to destroy the function of endothelial cells and result in vascular complications [36]. As a consequence, avoiding endothelial cell injury is the purpose of diabetic vascular complications therapy. A spate of reports show that lncRNAs involved in the pathogenesis of various human diseases can work as decoys, guides, signals, or scaffolds to combine DNA, RNA, or protein and consequently exert diverse biological functions [16]. According to our study, 3BDO inhibited high glucose-induced VEC autophagy and

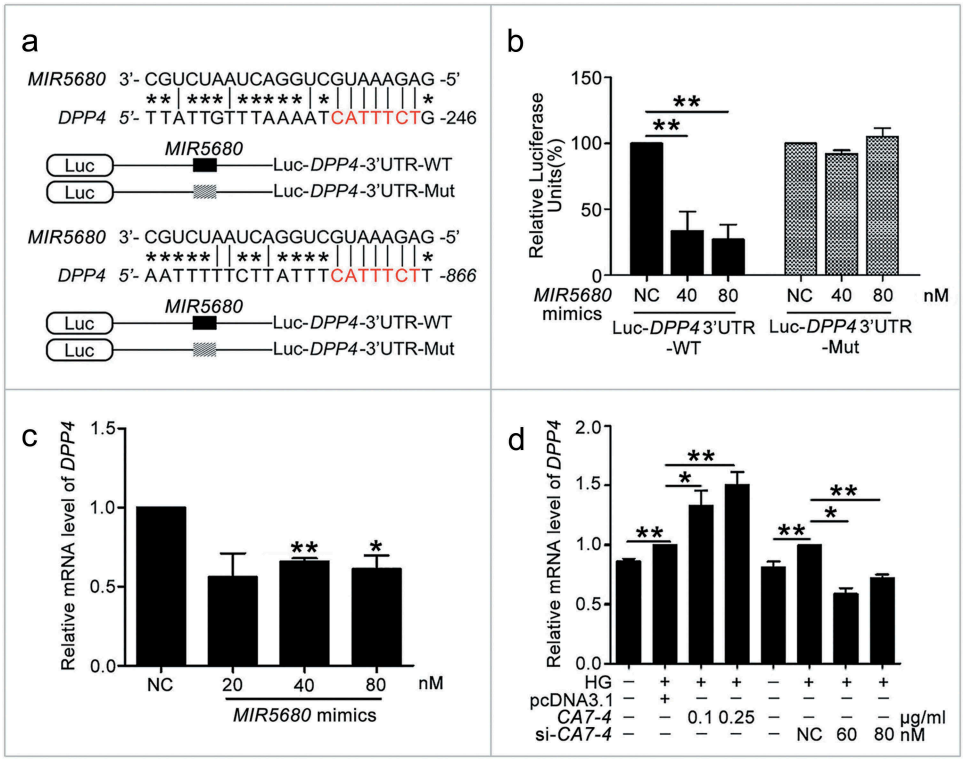

Figure 8. *MIR5680* targeted DPP4 and decreased the mRNA level of it. (a) Possible binding sites of *MIR5680* in *DPP4* 3′ UTR. (b) Luc-*DPP4* 3′ UTR-WT or Luc-*DPP4* 3′ UTR-Mut plasmids were co-transfected with NC or *MIR5680* mimics into HEK293T cells for 24 h. Luciferase activity was determined. (c) After transfection with NC, *MIR5680* mimics for 48 h, detecting the mRNA level of *DPP4* by qPCR analysis. (d) VECs were treated with HG for 48 h after overexpression or knockdown of *CA7-4*. qPCR analysis of *DPP4* mRNA level. (*, $p < 0.05$; **, $p < 0.01$; $n = 3$.).

apoptosis (Figure S1). LncRNA *CA7-4*, which was upregulated by high glucose, could be supressed by 3BDO (Figure 1). The function of *CA7-4* lacks evidence, particularly in endothelial cells during the development of hyperglycemia. We found that high glucose-induced autophagy and apoptosis of VECs sharpened with overexpression of *CA7-4* and its knockdown had the reverse effect (Figures 2, 3).

A number of lncRNAs are dysregulated in vascular cells under the circumstance of high glucose [37]. However, most have been identified to participate in regulating vascular dysfunction, as well as vascular apoptosis and inflammation, with no study about lncRNA regulating high glucose-induced VEC autophagy. Therefore, *CA7-4* discovered to promote VEC autophagy and apoptosis is of significance.

LncRNAs can function as ceRNAs. The crosstalk between lncRNAs, miRNAs and mRNA targets represents a complex network of gene expression regulation [38]. Hence, to explore the mechanism of *CA7-4* regulation in high glucose-induced VEC autophagy and apoptosis, we used bioinformatics prediction and searched for miRNAs that *CA7-4* might combine with. Further study showed that *CA7-4* could decoy *MIR877-3P* and *MIR5680*, and the levels of *MIR877-3P* and *MIR5680* were increased after treatment with 3BDO (Figure 4).

Previous study indicates that according to miRNA profiling, *MIR877-3P* is upregulated in earlier type II diabetic kidney disease [39]. *MIR877-3P* also plays important roles in else several diseases, including nephropathy [40], lung fibrosis [41], bladder cancer [42] and inflammatory [43]. However, the effect of *MIR877-3P* on VEC damage induced by high glucose had not been studied. Additionally, there were no reports on *MIR5680* functions. Here, *MIR877-3P* and *MIR5680* prevented VEC autophagy and apoptosis with or without high glucose treatment (Figures 5, 6, S6, S7). Then we predicted and detected the target genes of *MIR877-3P* and *MIR5680* (Table S1). The data suggested that *MIR877-3P* and *MIR5680* targeted *CTNNBIP1* (Figure 7) and *DPP4* (Figures 8, 9), respectively, and inhibited their expression at the transcription and translation levels, whereas *CA7-4* weakened the functions of *MIR877-3P* (Figure 7(d,g)) and *MIR5680* (Figures 8(d), 9(c)). In addition, treatment with si-*CA7-4* and 3BDO decreased the upregulation of CTNNBIP1 and DPP4 induced by high glucose (Figure S8).

CTNNBIP1 induces cell apoptosis by suppressing CTNNB1 activity [44], but no study has investigated the relationship between CTNNBIP1 and autophagy. DPP4, also known as CD26, can be expressed as a soluble enzyme in vascular beds including endothelial cells [45]. GLP1 (Glucagon like peptide-1), a substrate that belongs to DPP4, can promote insulin secretion and reduce glucagon production as a kind of incretin hormone. The increased DPP4 level leads to hyperglycemia by suppressing GLP1 [46]. As a kind of DPP4 inhibitor, sitagliptin reduces high glucose-caused apoptosis by activating AMPK in endothelial cells [47]. As well, sitagliptin alleviates hypoxia-induced autophagy and apoptosis by suppressing DPP4 to protect mesenchymal stem cells [32]. So, we investigated how DPP4 affected AMPK activity during VEC autophagy and apoptosis caused by high glucose.

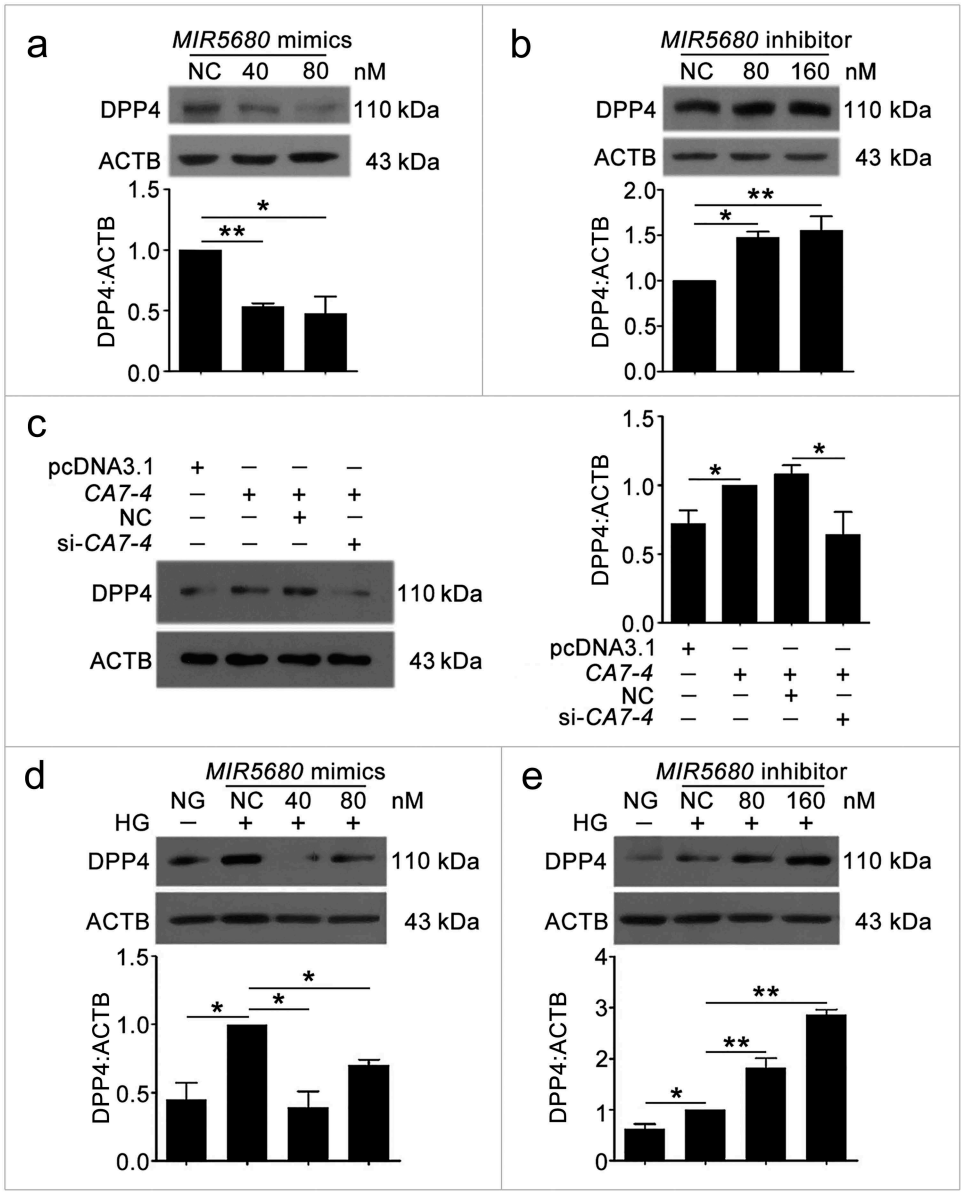

Figure 9. The protein level of DPP4 was negatively regulated by *MIR5680*. (a,b) VECs were transfected with *MIR5680* mimics or inhibitor for 48 h. (c) VECs were transfected with pcDNA3.1 or *CA7-4* (0.1 μg/ml); co-transfected with *CA7-4* (0.1 μg/ml) and NC or si-*CA7-4* (60 nM) for 48 h. (d,e) After transfection with NC, *MIR5680* mimics or inhibitor overnight, VECs were treated with HG for 48 h. Western blot analysis of DPP4 level. (*, $p < 0.05$; **, $p < 0.01$; n = 3.).

First, we analyzed whether *MIR877-3P* affected the expression of CTNNB1 and whether *MIR5680* affected AMPK phosphorylation. *MIR877-3P* or 3BDO increased the level of CTNNB1, and *CA7-4* downregulated it (Figure S9). The phosphorylation of AMPK was inhibited by *MIR5680* or 3BDO, and overexpression *CA7-4* reversed the result (Figure S10). To understand how CTNNBIP1 and DPP4 affect high glucose-induced VEC autophagy and apoptosis, we transfected cells with si-*CTNNBIP1* and si-*DPP4*. CTNNBIP1 and DPP4 knockdown reduced VEC autophagy and apoptosis under HG (Figure 10). Hence, we found novel pathways regulating VEC autophagy and apoptosis: *MIR877-3P*/CTNNBIP1/CTNNB1 and *MIR5680*/DPP4/AMPK.

In summary, under high glucose, 3BDO attenuates VEC autophagy and apoptosis by weakening the upregulation of *CA7-4*. As a ceRNA, *CA7-4* decoys *MIR877-3P* and *MIR5680*, promotes the expression of CTNNBIP1 and DPP4, decreases the level of CTNNB1 and increases AMPK phosphorylation, thereby aggravating VEC autophagy and apoptosis (Figure 11). Therefore, *CA7-4* might become an attractive target against autophagy and apoptosis of vascular endothelial cells.

Materials and methods

Cell culture

Source of VECs from human umbilical vein was consistent with the previous description [48]. The VECs were grown in M199 medium (Gibco, 31100-035) with 10% (V/V) bovine calf serum (Sigma-Aldrich, 13063C) and 8.4 IU/mL FGF2. HEK293T cells stemed from the Cell Bank of the Chinese Academy of Sciences (Shanghai) and grew in DMEM-H medium (Gibco, 12800017) with 10% fetal bovine serum (Gibco,

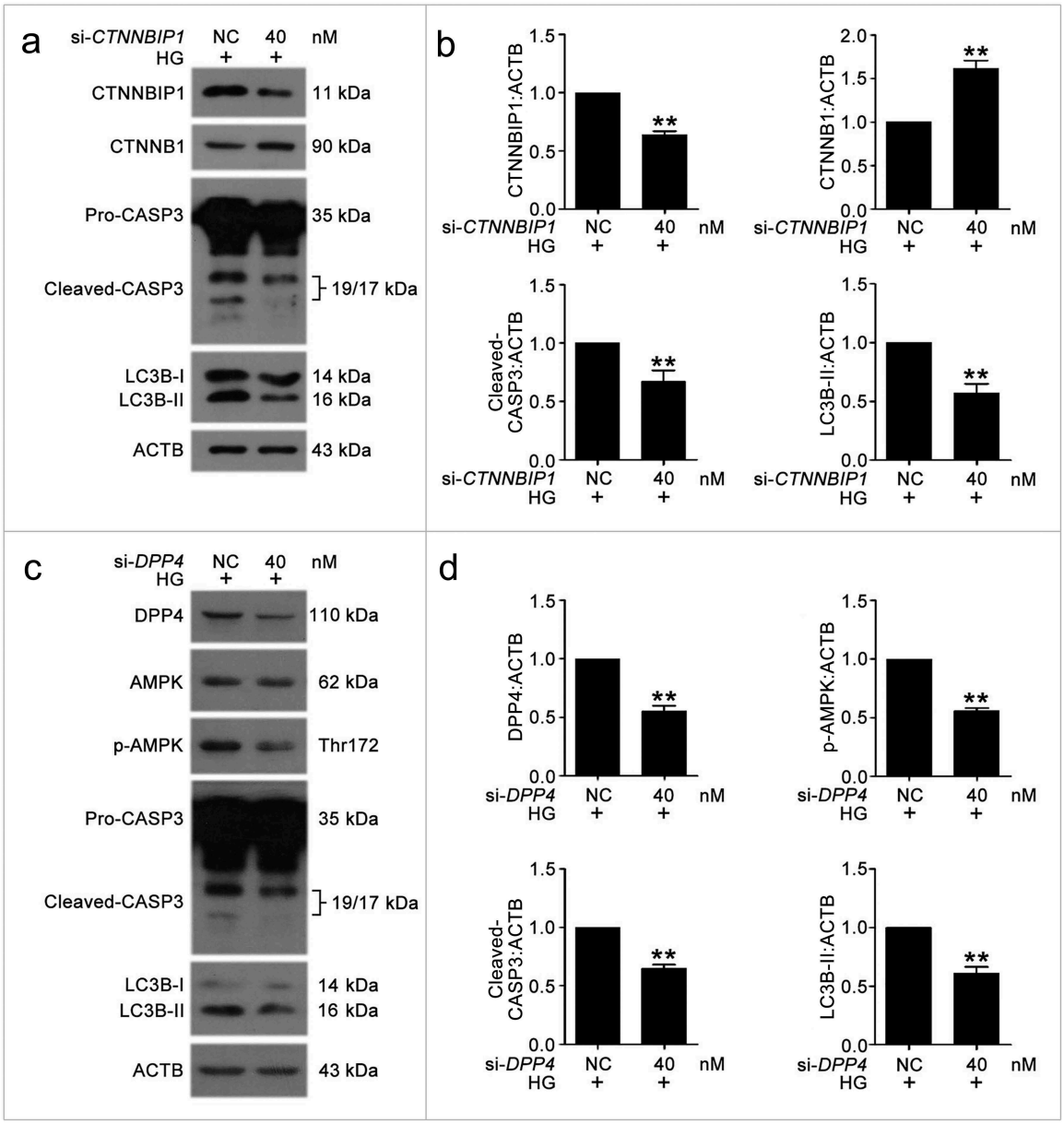

Figure 10. The knockdown of CTNNBIP1 and DPP4 reduced VEC autophagy and apoptosis caused by high glucose. (a–d) After transfection with NC, si-*CTNNBIP1* or si-*DPP4* overnight, VECs were treated with high glucose for 48 h. The protein levels of CTNNBIP1, CTNNB1, cleaved-CASP3, LC3B-II, DPP4, p-AMPK were analyzed by western blot. (*, $p < 0.05$; **, $p < 0.01$; n = 3.).

10270-106). H9C2, HepG2, PC3 and U87 cells were grown in DMEM-H medium with 10% fetal bovine serum. Hela cells were grown in DMEM-H medium with 10% bovine calf serum. A549 cells were grown in RPMI-1640 (Gibco, 31800089) medium with 10% bovine calf serum. HCT116 and THP-1 cells were grown in RPMI-1640 medium with 10% fetal bovine serum. All cell lines were cultured in a humidified incubator at 37°C with 5% CO_2.

Immunofluorescence assay

Immunofluorescence assay was performed as described previously [49]. First, VECs were fixed with 4% paraformaldehyde for 15 min and washed 3 times with 0.1 M phosphate-buffered saline (PBS: 137 mM NaCl, 2.7 mM KCl, 10 mM Na_2HPO_4, 2 mM KH_2PO_4, pH 7.4), then permeabilized with 0.1% Triton X-100 (Sangon Biotech, A600198). Cells were washed 3 times with 0.1 M PBS. At room temperature, 10% normal donkey serum (Solarbio, SL050) was applied to block cells for 20 min. Then VECs were incubated with LC3B primary antibody (1:100) (Cell Signaling Technology, 2775S) at 4°C overnight and corresponding secondary antibody (1:200) at 37°C for 1 h. Cells were washed 3 times with 0.1 M PBS. After treatment with DAPI (4', 6-diamidino-2-phenylindole) (Sigma-Aldrich, D8417) for 10 min, cells were washed 3 times with 0.1 M PBS, then photographed by confocal fluorescence microscopy Zeiss LSM700 (Germany).

Western blot analysis

Cells were lysed in RIPA lysis buffer (Beyotime, P0013B) containing protease inhibitor cocktail (Sigma-Aldrich, P8340) after being washed twice with 0.1 M PBS. Lysates

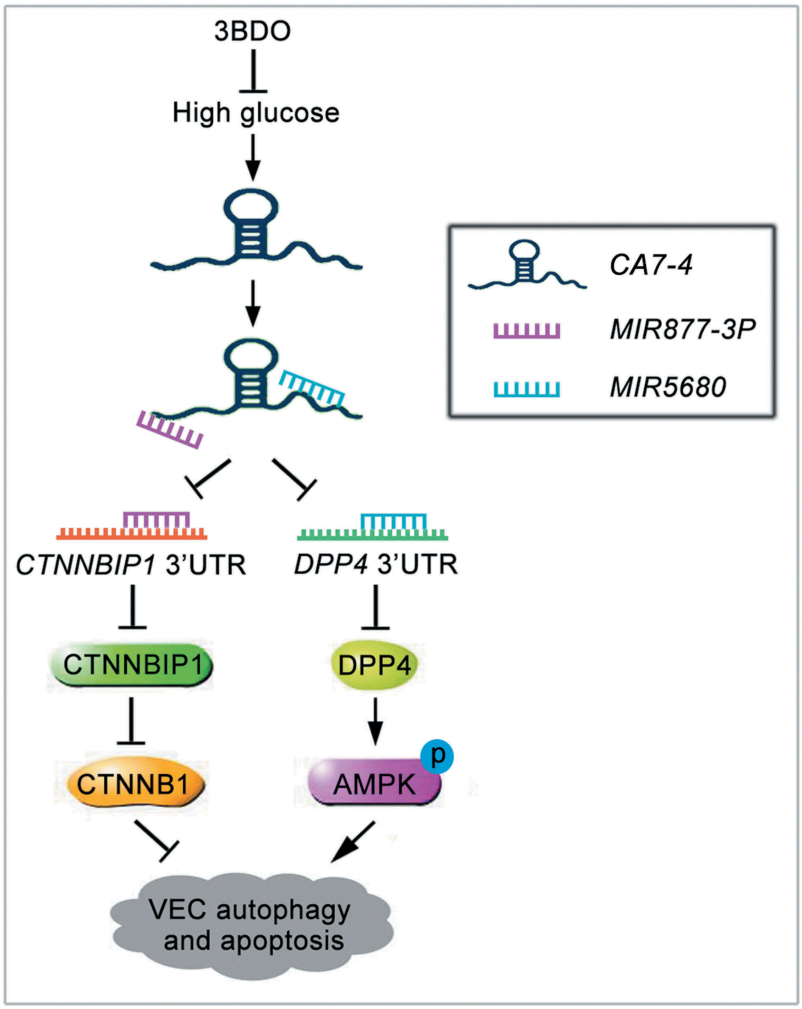

Figure 11. Schematic of *CA7-4* regulating VEC autophagy and apoptosis caused by high glucose. High glucose induces VEC autophagy and apoptosis. In this progress, upregulated *CA7-4* as a miRNA sponge to decoy *MIR877-3P* and *MIR5680*, promote the expression of CTNNBIP1 and DPP4, decrease the level of CTNNB1 and increase AMPK phosphorylation. 3BDO can attenuate high glucose-induced VEC autophagy and apoptosis by weakening the upregulation of *CA7-4*.

were centrifuged at 12,000 × g, 4°C for 15 min, collecting supernatant. Bicinchoninic acid (BCA) protein assay kit (Beyotime, P0011) was used for measuring protein concentration. After 15% or 12% SDS-PAGE at 4°C, protein was transferred to polyvinylidene difluoride (PVDF) membrane (Millipore, IPFL00010). The membrane was blocked with 5% non-fat milk for 1 h at room temperature, incubated with primary antibodies: PARP1 (Cell Signaling Technology, 9542S); LC3B (Cell Signaling Technology, 2775S); BCL2 (Proteintech, 12789-1-AP); BAX (Proteintech, 50599-2-Ig); CASP3 (Cell Signaling Technology, 9662S); ACTB (Sigma-Aldrich, A-5441); DPP4 (Abcam, ab215711); AMPK (Cell Signaling Technology, 5832S); p-AMPK (Cell Signaling Technology, 2535S); SQSTM1 (BD, 610833); CTNNBIP1 (Abcam, ab129011); CTNNB1 (Proteintech, 51067-2-AP), 1:1000 in TBS-Tween 20 (0.1%) at 4°C overnight (0.1 M TBS: 3 g Tris, 0.2 g KCl, 8 g NaCl, pH 7.4), washed TBST three times, then incubated with horseradish peroxidase-conjugated secondary antibodies (Jackson ImmunoResearch, goat anti-rabbit: 111-035-003, goat anti-mouse: 115-035-003) for 1 h at room temperature. Fluorescence signals were detected by X-ray films after being incubated with HRP substrate for 3 min. The expression of protein was quantified by ImageJ software.

Quantitative real-time PCR

Total RNA was purified by means of Trizol reagent (TAKARA, 9109). PARIS™ Kit (Invitrogen, AM1921) was utilized to isolate nuclear and cytoplasmic RNA according to the manufacturer's instructions. Following the PrimeScript RT reagent kit's (TAKARA, DRR047) protocol, RNA (1 μg) was reverse-transcribed to cDNA. Quantitative real-time PCR was implemented in a 20 μl volume containing 10 μl EvaGreen 2 × qPCR MasterMix (Applied Biological Materials, MasterMix-S), forward primer, reverse primer, template DNA, and nuclease-free H_2O. Relative gene expression was normalized to that of actin beta. Additionally, the levels of *MIR877-3P, MIR5680, MIR4778-3P* and *MIR561-3P* were analyzed by Hairpin-it microRNA and *RNU6* snRNA Normalization RT-PCR Quantitation Kit (GenePharma, E22001-E22010). Relative gene expression was normalized to that of *RNU6* snRNA. Primer information is provided in the supplemental material.

Transient transfection

CA7-4 overexpression full-length plasmid (pcDNA3.1-*CA7-4*) was obtained by inserting the full length of *CA7-4* into pcDNA3.1 vector. Control: pcDNA3.1-empty vector. Specific small interfering RNAs, including *CA7-4, CTNNBIP1, DPP4*, scramble siRNA (negative control); miRNA mimics and inhibitors for *MIR877-3P, MIR5680, MIR4778-3P*, and *MIR561-3P* were designed and synthesized by Invitrogen. Plasmids were transfected by using Lipofectamine 2000 (Invitrogen, 11668-019) according to protocols. In addition, siRNAs, miRNA mimics and inhibitor were transfected by using HiPerFect Transfection Reagent (QIAGEN, 301705) according to the manufacturer's instructions.

Hoechst 33258 staining

After treatment, VECs grown on 24 well plates were stained with 10 mg/ml Hoechst 33258 (Sangon Biotech, E607329) at 37°C for 15 min, avoid light. Cells were washed with PBS twice and photographed by using a fluorescence microscope (Japan).

Luciferase activity assay

Luciferase reporter plasmids were reconstructed by inserting target fragments into pmirGLO Dual-Luciferase miRNA Target Expression Vectors (dual-luciferase: firefly luciferase and renilla luciferase). Dual luciferase reporter plasmids of Luc-*CA7-4*-WT, Luc-*CA7-4-MIR877-3P* or *MIR5680* or *MIR4778-3P* or *MIR561-3P*-Mut, Luc-*CTNNBIP1* or *DPP4*-3′ UTR-WT, Luc-*CTNNBIP1* or *DPP4*-3′ UTR-Mut, were used in the experiments. HEK293T cells were cultured onto 96-well plates at 10000 cells per well overnight in DMEM-H medium (Gibco, 12800017) with 10% fetal bovine serum, then co-transfected with plasmids of dual-luciferase reporters and miRNA mimics or NC, detecting dual-luciferase activity by using the Dual-Glo Luciferase Assay System Kit (Promega, E2920) according to the instructions. Firefly luciferase activity was normalized to renilla luciferase activity.

TUNEL assay

TUNEL assay was performed by using In Situ Cell Detection Kit (Roche Applied Science, 11767291910) according to the manufacturer's instructions and photographed by laser scanning confocal microscopy (Zeiss LSM700, Germany).

RNA-binding protein immunoprecipitation (RIP) assay

RIP assay was operated with the Magna RIP RNA-Binding Protein Immunoprecipitation Kit (Millipore, 17-701). Briefly, VECs were lysed, and incubated with magnetic beads conjugated with human anti-AGO2 antibody (Millipore, 03-110) or anti-mouse IgG (Millipore, 03-110). The immunoprecipitated RNA was detected by qPCR.

Statistical analysis

Experimental data are shown as means ± SEM from at least three independent experiments and were analyzed by using SPSS 17.0 (SPSS Inc., Chicago, IL, USA). $P < 0.05$ was considered statistically significant.

Highlights

- A small chemical molecule — 3 - benzyl −5 - ((2-nitrophenoxy) methyl) - dihydrofuran-2 (3H) - one (3BDO) — synthesized by us could simultaneously inhibit autophagy and apoptosis induced by a high concentration of glucose in vascular endothelial cells (VECs).
- A novel long noncoding RNA called *CA7-4* could promote VEC autophagy and apoptosis triggered by high glucose; 3BDO inhibited the role of *CA7-4*.
- *CA7-4* directly bonded with *MIR877-3P* and *MIR5680* as a decoy.
- We confirmed that *MIR877-3P* and *MIR5680* targeted 3′UTRs of *CTNNBIP1* and *DPP4*, respectively.
- *MIR877-3P* inhibited high glucose-induced VEC autophagy and apoptosis by decreasing the expression of CTNNBIP1 and upregulating CTNNB1.
- *MIR5680* protected VECs against high glucose-induced autophagy and apoptosis by targeting DPP4 and weakening PRKAA1 phosphorylation.
- Therefore, *CA7-4, MIR877-3P* and *MIR5680* represent novel signal pathways regulating high glucose-induced autophagy and apoptosis in VECs.

Disclosure statement

No potential conflict of interest was reported by the authors.

Funding

This work was supported by the National Natural Science Foundation of China (No. 91539105, 81321061, 91313303).

References

[1] Eelen G, de Zeeuw P, Simons M, et al. Endothelial cell metabolism in normal and diseased vasculature. Circ Res. 2015 Mar 27;116 (7):1231–1244. PubMed PMID: 25814684; PubMed Central PMCID: PMC4380230.

[2] Zaitseva II, Berggren PO, Zaitsev SV. Insulinotropic compounds decrease endothelial cell survival. Toxicol In Vitro. 2016 Jun;33:1–8. PubMed PMID: 26883446.

[3] Zhu M, Wen M, Sun X, et al. Propofol protects against high glucose-induced endothelial apoptosis and dysfunction in human umbilical vein endothelial cells. Anesth Analg. 2015 Apr;120(4):781–789. PubMed PMID: 25793913.

[4] Zhao Q, Gao C, Cui Z. Ginkgolide A reduces inflammatory response in high-glucose-stimulated human umbilical vein endothelial cells through STAT3-mediated pathway. Int Immunopharmacol. 2015 Apr;25(2):242–248. PubMed PMID: 25681539.

[5] Jayakumar T, Chang CC, Lin SL, et al. Brazilin ameliorates high glucose-induced vascular inflammation via inhibiting ROS and CAMs production in human umbilical vein endothelial cells.

Biomed Res Int. 2014;2014:403703. PubMed PMID: 24716195; PubMed Central PMCID: PMC3955648.
[6] Chen F, Chen B, Xiao FQ, et al. Autophagy protects against senescence and apoptosis via the RAS-mitochondria in high-glucose-induced endothelial cells. Cell Physiol Biochem. 2014;33(4):1058–1074. PubMed PMID: 24732710.
[7] Sallam T, Sandhu J, Tontonoz P. Long noncoding RNA discovery in cardiovascular disease: decoding form to function. Circ Res. 2018 Jan 5;122(1):155–166. PubMed PMID: 29301847.
[8] Jandura A, Krause HM. The new RNA world: growing evidence for long noncoding RNA functionality. Trends Genet. 2017 Oct;33 (10):665–676. PubMed PMID: 28870653.
[9] Fok ET, Scholefield J, Fanucchi S, et al. The emerging molecular biology toolbox for the study of long noncoding RNA biology. Epigenomics. 2017 Oct;9(10):1317–1327. PubMed PMID: 28875715.
[10] Li L, Chen H, Gao Y, et al. Long noncoding RNA MALAT1 promotes aggressive pancreatic cancer proliferation and metastasis via the stimulation of autophagy. Mol Cancer Ther. 2016 Sep;15(9):2232–2243. PubMed PMID: 27371730.
[11] Chen CL, Tseng YW, Wu JC, et al. Suppression of hepatocellular carcinoma by baculovirus-mediated expression of long non-coding RNA PTENP1 and MicroRNA regulation. Biomaterials. 2015 Mar;44:71–81. PubMed PMID: 25617127.
[12] Schmitz SU, Grote P, Herrmann BG. Mechanisms of long noncoding RNA function in development and disease. Cell Mol Life Sci. 2016 Jul;73(13):2491–2509. PubMed PMID: 27007508; PubMed Central PMCID: PMC4894931.
[13] Ballantyne MD, McDonald RA, Baker AH. lncRNA/MicroRNA interactions in the vasculature. Clin Pharmacol Ther. 2016 May;99 (5):494–501. PubMed PMID: 26910520; PubMed Central PMCID: PMC4881297.
[14] Wang K, Liu CY, Zhou LY, et al. APF lncRNA regulates autophagy and myocardial infarction by targeting miR-188-3p. Nat Commun. 2015 Apr 10;6:6779. PubMed PMID: 25858075.
[15] Viereck J, Kumarswamy R, Foinquinos A, et al. Long noncoding RNA chast promotes cardiac remodeling. Sci Transl Med. 2016 Feb 17;8(326):326ra22. PubMed PMID: 26888430.
[16] Leti F, DiStefano JK. Long noncoding RNAs as diagnostic and therapeutic targets in type 2 diabetes and related complications. Genes. 2017 Aug 22;8(8):207. PubMed PMID: 28829354; PubMed Central PMCID: PMC5575670.
[17] Liu JY, Yao J, Li XM, et al. Pathogenic role of lncRNA-MALAT1 in endothelial cell dysfunction in diabetes mellitus. Cell Death Dis. 2014 Oct 30;5:e1506. PubMed PMID: 25356875; PubMed Central PMCID: PMC4649539.
[18] Qiu GZ, Tian W, Fu HT, et al. Long noncoding RNA-MEG3 is involved in diabetes mellitus-related microvascular dysfunction. Biochem Biophys Res Commun. 2016 Feb 26;471(1):135–141. PubMed PMID: 26845358.
[19] Yan B, Yao J, Liu JY, et al. lncRNA-MIAT regulates microvascular dysfunction by functioning as a competing endogenous RNA. Circ Res. 2015 Mar 27;116(7):1143–1156. PubMed PMID: 25587098.
[20] Zhang B, Wang D, Ji TF, et al. Overexpression of lncRNA ANRIL up-regulates VEGF expression and promotes angiogenesis of diabetes mellitus combined with cerebral infarction by activating NF-kappaB signaling pathway in a rat model. Oncotarget. 2017 Mar 7;8(10):17347–17359. PubMed PMID: 28060742; PubMed Central PMCID: PMC5370045.
[21] Nemecz M, Alexandru N, Tanko G, et al. Role of MicroRNA in endothelial dysfunction and hypertension. Curr Hypertens Rep. 2016 Dec;18(12):87. PubMed PMID: 27837398.
[22] Tang ST, Wang F, Shao M, et al. MicroRNA-126 suppresses inflammation in endothelial cells under hyperglycemic condition by targeting HMGB1. Vascul Pharmacol. 2017 Jan;88:48–55. PubMed PMID: 27993686.
[23] Yuan J, Chen M, Xu Q, et al. Effect of the diabetic environment on the expression of MiRNAs in endothelial cells: mir-149-5p restoration ameliorates the high glucose-induced expression of TNF-α and ER stress markers. Cell Physiol Biochem. 2017;43 (1):120–135. PubMed PMID: 28848152.
[24] Zhang Y, Sun X, Icli B, et al. Emerging roles for MicroRNAs in diabetic microvascular disease: novel targets for therapy. Endocr Rev. 2017 Apr 1;2017(1):1–22. PubMed PMID: 28520942.
[25] Wang WW, Liu X, Zhao J, et al. A novel butyrolactone derivative inhibited apoptosis and depressed integrin β4 expression in vascular endothelial cells. Bioorg Med Chem Lett. 2007 Jan 15;17 (2):482–485. PubMed PMID: WOS:000244012200038; English.
[26] Ge D, Han L, Huang S, et al. Identification of a novel MTOR activator and discovery of a competing endogenous RNA regulating autophagy in vascular endothelial cells. Autophagy. 2014 Jun;10(6):957–971. PubMed PMID: 24879147; PubMed Central PMCID: PMC4091179.
[27] Huang S, Lu W, Ge D, et al. A new microRNA signal pathway regulated by long noncoding RNA TGFB2-OT1 in autophagy and inflammation of vascular endothelial cells. Autophagy. 2015;11 (12):2172–2183. PubMed PMID: 26565952; PubMed Central PMCID: PMC4835209.
[28] Gong Q, Su G. Roles of miRNAs and long noncoding RNAs in the progression of diabetic retinopathy. Biosci Rep. 2017 Dec 22;37 (6):BSR20171157. PubMed PMID: 29074557; PubMed Central PMCID: PMC5705777.
[29] Noh JH, Kim KM, McClusky WG, et al. Cytoplasmic functions of long noncoding RNAs. Wiley Interdiscip Rev RNA. 2018 May–Jun;9(3):e1471. PubMed PMID: WOS:000430472400007; English.
[30] Hossain MZ, Yu Q, Xu M, et al. ICAT expression disrupts beta-catenin-TCF interactions and impairs survival of thymocytes and activated mature T cells. Int Immunol. 2008 Jul;20 (7):925–935. PubMed PMID: 18511409; PubMed Central PMCID: PMC2556852.
[31] Deacon CF. A review of dipeptidyl peptidase-4 inhibitors. Hot topics from randomized controlled trials. Diabetes Obes Metab. 2018 Feb;20 Suppl 1:34–46. PubMed PMID: 29364584.
[32] Wang XM, Yang YJ, Wu YJ, et al. Attenuating hypoxia-induced apoptosis and autophagy of mesenchymal stem cells: the potential of sitagliptin in stem cell-based therapy. Cell Physiol Biochem. 2015;37(5):1914–1926. PubMed PMID: 26584290.
[33] Fu X, Zhu X, Qin F, et al. Linc00210 drives Wnt/β-catenin signaling activation and liver tumor progression through CTNNBIP1-dependent manner. Mol Cancer. 2018 Mar 14;17 (1):73. PubMed PMID: 29540185; PubMed Central PMCID: PMC5853034.
[34] Huang CN, Wang CJ, Lee YJ, et al. Active subfractions of Abelmoschus esculentus substantially prevent free fatty acid-induced β cell apoptosis via inhibiting dipeptidyl peptidase-4. PloS one. 2017;12(7):e0180285. PubMed PMID: 28715446; PubMed Central PMCID: PMC5513409.
[35] Yang F, Zhang L, Gao Z, et al. Exogenous H2S protects against diabetic cardiomyopathy by activating autophagy via the AMPK/mTOR pathway. Cell Physiol Biochem. 2017;43(3):1168–1187. PubMed PMID: 28977784.
[36] Chen X, Duong MN, Psaltis PJ, et al. High-density lipoproteins attenuate high glucose-impaired endothelial cell signaling and functions: potential implications for improved vascular repair in diabetes. Cardiovasc Diabetol. 2017 Sep 29;16(1):121. PubMed PMID: 28962618; PubMed Central PMCID: PMC5622442.
[37] Leung A, Amaram V, Natarajan R. Linking diabetic vascular complications with LncRNAs. Vascul Pharmacol. 2018 Feb 1;114:139–144. PubMed PMID: 29398367; PubMed Central PMCID: PMC6070440.
[38] Tay Y, Rinn J, Pandolfi PP. The multilayered complexity of ceRNA crosstalk and competition. Nature. 2014 Jan 16;505 (7483):344–352. PubMed PMID: 24429633; PubMed Central PMCID: PMC4113481.
[39] Xie Y, Jia Y, Cuihua X, et al. Urinary exosomal MicroRNA profiling in incipient type 2 diabetic kidney disease. J Diabetes Res. 2017;2017:6978984. PubMed PMID: 29038788; PubMed Central PMCID: PMC5605810.

[40] Liang Y, Zhao G, Tang L, et al. Corrigendum to "MiR-100-3p and miR-877-3p regulate overproduction of IL-8 and IL-1beta in mesangial cells activated by secretory IgA from IgA nephropathy patients" [Exp. Cell Res. 347 (2016) 312-321]. Exp Cell Res. 2016 Nov 15;349(1):198. PubMed PMID: 27745865.

[41] Wang C, Gu S, Cao H, et al. miR-877-3p targets Smad7 and is associated with myofibroblast differentiation and bleomycin-induced lung fibrosis. Sci Rep. 2016 Jul 22;6:30122. PubMed PMID: 27444321; PubMed Central PMCID: PMC4957095.

[42] Li S, Zhu Y, Liang Z, et al. Up-regulation of p16 by miR-877-3p inhibits proliferation of bladder cancer. Oncotarget. 2016 Aug 9;7 (32):51773–51783. PubMed PMID: 27429046; PubMed Central PMCID: PMC5239514.

[43] Williams AE, Choi K, Chan AL, et al. Sjogren's syndrome-associated microRNAs in CD14+ monocytes unveils targeted TGFβ signaling. Arthritis Res Ther. 2016 May 3;18(1):95. PubMed PMID: 27142093; PubMed Central PMCID: PMC4855899.

[44] Zhang K, Zhu S, Liu Y, et al. ICAT inhibits glioblastoma cell proliferation by suppressing Wnt/β-catenin activity. Cancer Lett. 2015 Feb 1;357(1):404–411. PubMed PMID: 25434796.

[45] Mulvihill EE, Drucker DJ. Pharmacology, physiology, and mechanisms of action of dipeptidyl peptidase-4 inhibitors. Endocr Rev. 2014 Dec;35(6):992–1019. PubMed PMID: 25216328.

[46] Rahimi N, Samavati Sharif MA, Goharian AR, et al. The effects of aerobic exercises and 25(OH) D supplementation on GLP1 and DPP4 level in type II diabetic patients. Int J Prev Med. 2017;8:56. PubMed PMID: 28900535; PubMed Central PMCID: PMC5582496.

[47] Wu C, Hu S, Wang N, et al. Dipeptidyl peptidase4 inhibitor sitagliptin prevents high glucoseinduced apoptosis via activation of AMPactivated protein kinase in endothelial cells. Mol Med Rep. 2017 Jun;15(6):4346–4351. PubMed PMID: 28440488.

[48] Jaffe EA, Nachman RL, Becker CG, et al. Culture of human endothelial cells derived from umbilical veins. Identification by morphologic and immunologic criteria. J Clin Invest. 1973 Nov;52 (11):2745–2756. PubMed PMID: 4355998; PubMed Central PMCID: PMC302542.

[49] Zhao X, Dong W, Gao Y, et al. Novel indolyl-chalcone derivatives inhibit A549 lung cancer cell growth through activating Nrf-2/HO-1 and inducing apoptosis in vitro and in vivo. Sci Rep. 2017 Jun 20;7(1):3919. PubMed PMID: 28634389; PubMed Central PMCID: PMC5478673.